nature portfolio

Peer Review File

Nanoscale Heterophase Regulation Enables Sunlight-like Full-spectrum White Electroluminescence

Corresponding Author: Professor Haibo Zeng

This manuscript has been previously reviewed at another journal. This document only contains information relating to versions considered at Nature Communications.

Parts of this Peer Review File have been redacted as indicated to remove third-party material.

This file contains all reviewer reports in order by version, followed by all author rebuttals in order by version.

Version 1:

Reviewer comments:

Reviewer #1

(Remarks to the Author)
In the response and the revised manuscript, the authors have addressed the minor issues raised in my previous reviews, while the key concerns remain unaddressed. Therefore, I am still not convinced that this work is a significant breakthrough compared to the authors' previous study. Additionally, there are contradictory statements, and several claims lack sufficient evidence.
1. Both works are based on hetero phases of CsPbI3. The authors claim that the previous work involved an α/δ-phase mixture, while this study involves a γ/δ-phase mixture. However, the evidence provided is unclear. The authors only present raw GIWAXS (Fig. 2d-g) and XRD data (Fig. S9 and S10), and it is not clear whether these data actually support their claims. Although the authors include HRTEM images, these images do not reveal any clear heterophases.
2. The authors claim that they have achieved a more balanced carrier distribution. However, there is no evidence to support this claim. Furthermore, if the carrier distribution is indeed more balanced compared to the authors' previous work, the device performance should be higher. I regret to say that I still do not consider this work significant, given the poor device performance.
3. How about the performance of small-area devices? The authors used nearly identical spin coating parameters in this study. Why, then, did they achieve better large-area films in this work compared to their previous study?

Reviewer #2

(Remarks to the Author)
We thank the authors for their efforts in addressing our comments. However, after reviewing the revised manuscript and the responses to the reviewers, I still have some concerns.
Comment 1: The authors mention that different instruments were used to test the white LEDs and CsPbI3-based LED devices. We strongly recommend using the same testing instrument for comparison, as this may help to eliminate abnormal peaks.
Comment 2: The lifetime of white LEDs is critical. According to Figure R4, there is no obvious change in intensity or spectral shape, indicating that the device has good operating stability. Typically, the duration of the lifetime test for LEDs should be extended to T50. We recommend extending the testing duration and comparing the results with previously reported works in terms of lifetime.
Comment 3: The authors claim: “The α-phase will spontaneously undergo a phase transition to the β-phase, then to the γ-phase, and finally to the δ-phase at room temperature,” and “Joule heat generation during operation promotes the phase transition from the γ-phase to the δ-phase.” So, will the γ/δ-CsPbI3 film eventually transform entirely into the δ-phase during long-term operation? Please provide more experiment results and discussion.

Version 2:

Reviewer comments:

Reviewer #1

(Remarks to the Author)
In the response letter and the revised manuscript, the authors have addressed my concerns. I suggest the authors add the data of small-area devices in the supplementary information.

Reviewer #2

(Remarks to the Author)
We have carefully reviewed the revised manuscript; however, several concerns still need to be addressed:
1. The authors presented the stability result, showing a T50 of 220 minutes. Based on this result, we have concerns about the EL spectrum evolution in Fig. S25, which indicates no degradation in EL intensity. Please clarify the discrepancy between these two results.
2. In the revised manuscript, the authors mentioned the device invalidation stage. However, they did not specify when the invalidation occurred—was it before or after T50? Please add spectrum change data over the entire operating time.
3. The authors have still not addressed our question regarding the phase transition during operation. Please investigate and test the phase transition during continuous operation, as this will help elucidate the mechanism of device invalidation.
4. The T50 of the device remains far from meeting the requirements for practical applications. Please include a more in-depth discussion on this point and provide suggestions or strategies for improving the stability of the device.

Version 3:

Reviewer comments:

Reviewer #2

(Remarks to the Author)
The authors have addressed my concerns. I think the manuscript is ready for publication.

We appreciate reviewers' helpful comments and suggestions and have replied to them point by point in the following content. For clarity, reviewers' original comments and our response are in blue fonts, and the changes we made to the main text are quoted in *red fonts*. We have also highlighted the corresponding modifications in yellow in the revised manuscript.

Replies to Reviewer #1

Comments to the Author:

In the response and the revised manuscript, the authors have addressed the minor issues raised in my previous reviews, while the key concerns remain unaddressed. Therefore, I am still not convinced that this work is a significant breakthrough compared to the authors' previous study. Additionally, there are contradictory statements, and several claims lack sufficient evidence.

Comment 1: Both works are based on hetero phases of $CsPbI_3$. The authors claim that the previous work involved an α/δ-phase mixture, while this study involves a γ/δ-phase mixture. However, the evidence provided is unclear. The authors only present raw GIWAXS (Fig. 2d-g) and XRD data (Fig. S9 and S10), and it is not clear whether these data actually support their claims. Although the authors include HRTEM images, these images do not reveal any clear heterophases.

Response: Thanks for your comments. The previous report did not focus on the specific structure of the black phase, while in this manuscript, we clarified the black phase structure in the heterophase film for the first time. The GIWAXS and XRD measurements cannot clarify the specific phase because the three black phases have similar structural properties. **Thus, in this work, we performed scanning electron diffraction (SED) measurements to confirm the phase structure, which is important for designing the heterophase composition and further analysis of the carrier transport mechanism.**

Electron diffraction is a powerful tool for characterising the structural properties of materials and can be used to identify the specific nature of octahedral tilting in a given perovskite sample. In particular, in-phase and anti-phase octahedral tilts give rise to distinct Bragg peaks at different positions in the diffraction pattern. **By analysing the position and intensity of these peaks, it is possible to determine the type and degree of octahedral tilting present in the sample.** This information can be used to understand the underlying crystallographic structure and inform the design of new materials with desired properties. Glazer developed rules for superstructure reflections, which were applied to electron diffraction by Woodward et al. and form the basis of the current analysis.[1,2]

As discussed in our manuscript, the space groups for the black phase of halide perovskites, identified in the literature, are the following: $\boldsymbol{Pm\bar{3}m}$**,** ***P*4/*mbm*****, and** ***Pnma***. Stoumpos et al. reported that when cooled down from a high temperature, black-phase Pb-based and Sn-based halide perovskites showed a symmetry lowering via octahedral tilting.[3] They classified the three phases as α-phase (high temperature), β-phase (intermediate temperature) and γ-phase (low temperature), corresponding to $Pm\bar{3}m$, *P*4/*mbm*, and *Pnma*, respectively.[4] **In the halide perovskite literature, it is common to find assignments of α-phase cubic perovskite without rigorous determination of crystal symmetry.** Here, we simulate key zone axis electron diffraction patterns (ZADPs) of interest from these three tilt systems assigned in the literature and show that electron diffraction can be used to analyse the various types of octahedral tilts and differentiate between different tilt systems and in turn different structural phases (**Fig. R1**).

The $Pm\bar{3}m$ phase, which corresponds to a $a^o a^o a^o$ tilt system with no tilts about any of the three axes (**Fig. R1a**). The *P*4/*mbm* phase corresponds to a $a^o a^o c^+$ tilt system, with in-phase octahedral tilting about the c axis and no tilts about the a and b axes (**Fig. R1b**). The *Pnma* space group corresponds to a $a^- a^- c^+$ tilt system, with anti-phase tilts about the a and b axes and an in-phase tilt about the c axis (**Fig. R1c**).

In **Fig. R2a** (**Fig. 2c** in the revised manuscript), **we observed that diffraction rings**

correspond well to the diffracting planes of the γ-phase (*Pnma* perovskite). It can be found that the diffraction patterns from $Pm\bar{3}m$ and *Pnma* space groups for $<100>_c$ and $<110>_c$ are different, which is also confirmed by diffraction pattern results of α-phase in other reports (**Fig. R2b**, extracted from *Science* **374**, 1598-1605 (2021)). We also provided the HRTEM and Fourier transform pattern of α-phase (**Fig. R3**).

Besides, apart from the direct observational evidence of SED results, indirect evidence of optical properties could also confirm our conclusions (**Fig. R4**). The deep-red region in white EL showed a ~695 nm peak, while the PL peak of α-phase QD solution was located at ~684 nm. **The 11 nm redshift indicated the phase transition from α-phase to γ-phase.** All the other optical measurements were also consistent with this result.

All these results could clarify the phase composition of the heterophase film, which makes up for some deficiencies in the reported research and enriches the theoretical research of phase transition in the field.

As suggested, we have updated the corresponding content in the revised manuscript and highlighted it in yellow.

Page 7: *To understand the phase composition and structure of the heterophase films, we performed scanning electron diffraction (SED) measurements to identify the specific nature of octahedral tilting in a given perovskite sample.*

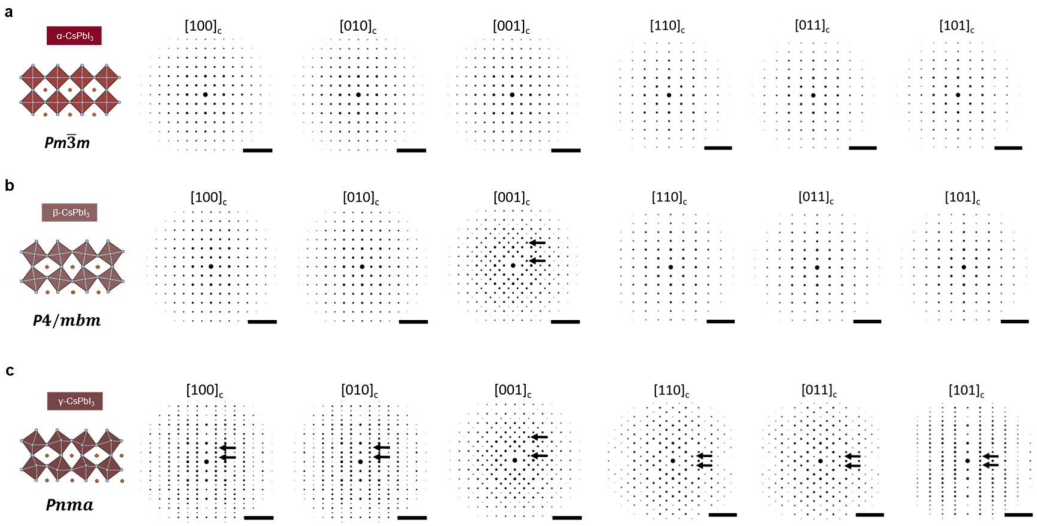

Fig. R1 Selection of simulated <100>$_c$ and <110>$_c$ diffraction patterns from $Pm\bar{3}m$, *P*4/*mbm* and *Pnma* space groups. **a**, Simulated $[100]_c$, $[010]_c$, $[001]_c$, $[110]_c$, $[011]_c$ and $[101]_c$ zone axis of $Pm\bar{3}m$. **b**, Simulated $[100]_c$, $[010]_c$, $[001]_c$, $[110]_c$, $[011]_c$ and $[101]_c$ zone axis of *P*4/*mbm*. **c**, Simulated $[100]_c$, $[010]_c$, $[001]_c$, $[110]_c$, $[011]_c$ and $[101]_c$ zone axis of *Pnma*. All scalebars are 0.5 $Å^{-1}$.

[FIGURE REDACTED]

Fig. R2 a, Annular dark field image of a region of interest. The scale bar is 0.6 $Å^{-1}$. **b**, The ED pattern of α-phase ($Pm\bar{3}m$) oriented near the $[001]_c$ zone axis. (**Fig. 2c** in manuscript) **c**, The ED pattern of α-phase ($Pm\bar{3}m$) oriented near the $[110]_c$ zone axis. The figures **b**, **c** were extracted from *Science* **374**, 1598-1605 (2021)

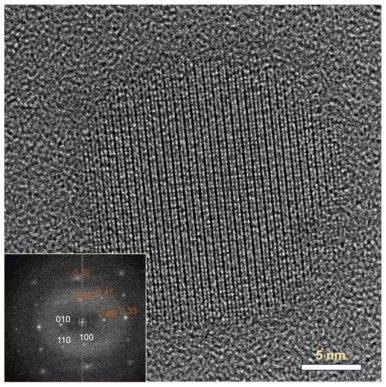

Fig. R3 HRTEM image and Fourier transform pattern of α-phase $CsPbI_3$ solution.

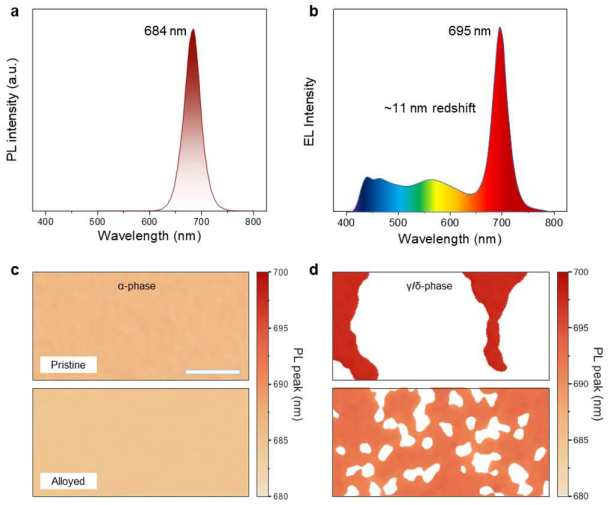

Fig. R4 a, PL spectrum of QD solution. b, EL spectrum of WLED. c, Hyperspectral images of α-$CsPbI_3$ and α-$CsPb(I/Cl)_3$ QDs film ranging from 660 to 700 nm. d, Hyperspectral images of the γ/δ-$CsPbI_3$ and γ/δ-$CsPb(I/Cl)_3$ film ranging from 660 to 700 nm. (**Fig. R4c, d** corresponding to **Fig. 3a, b** in the revised manuscript, respectively)

References:

1 Glazer, A. Simple ways of determining perovskite structures. *Acta Crystallographica Section A: Crystal Physics, Diffraction, Theoretical and General Crystallography* **31**, 756-762 (1975).

2 Woodward, D. I. & Reaney, I. M. Electron diffraction of tilted perovskites. *Acta Crystallographica Section B: Structural Science* **61**, 387-399 (2005).

3 Stoumpos, C. C., Malliakas, C. D. & Kanatzidis, M. G. Semiconducting tin and lead iodide perovskites with organic cations: phase transitions, high mobilities, and near-infrared photoluminescent properties. *Inorganic chemistry* **52**, 9019-9038 (2013).

4 Yamada, K. *et al.* Structural phase transitions of the polymorphs of CsSnI3 by means of

rietveld analysis of the X-ray diffraction. *Chem. Lett.*, 801-804 (1991).

Comment 2: The authors claim that they have achieved a more balanced carrier distribution. However, there is no evidence to support this claim. Furthermore, if the carrier distribution is indeed more balanced compared to the authors' previous work, the device performance should be higher. I regret to say that I still do not consider this work significant, given the poor device performance.

Response: We sincerely appreciate your comment. To achieve sunlight-like full-spectrum white EL, we need to **regulate the carrier distribution in different phases, even the carrier distribution in different energy levels in a single phase**. Besides, fabricating a large-area plane light source (traditional WLED is a point light source) is of practical significance for lighting applications, while **no large-area perovskite-based WLED has been reported so far**. This is mainly attributed to the difficulty of uniformity control in the large-area film along with the complex transport and distribution mechanism of carriers. Thus, balanced carrier distribution is difficult to obtain but important for achieving stable and balanced full-spectrum large-area white EL.

In this work, based on theoretical calculation results, we designed the alloyed γ/δ-$CsPb(I/Cl)_3$ system for balanced heterophase and carrier distribution (**Fig. R5a, b**). Then, we used hyperspectral wide-field microscopy, hyperspectral wide-field microscopy, temperature-dependent PL spectroscopy and EL spectrum results to confirm the balanced carrier distribution in our previous manuscript (**Fig. R5c-h**). Besides, in this round of revision, we have studied the evolution of EL during the invalidation stage of the device to confirm further the balanced carrier distribution (**Fig. R6**).

We will explain "balanced carrier distribution" in detail from the following aspects:

(1) Theoretical calculation

We investigated the relative stability between the γ- and δ-phase in the γ/δ-$CsPb(I/Cl)_3$ system by first-principles and thermodynamic calculations (**Fig. R5a, b**).

The Helmholtz free energy difference approaches zero at 33% Cl^- component at room temperature, indicating that alloyed γ/δ-$CsPb(I/Cl)_3$ system enables a more uniform heterophase distribution and feasible lattice twisting, providing the possibility for achieving tuneable full-spectrum white light.

(2) Optical properties

We employed hyperspectral wide-field microscopy to spatially map the heterophase film's photoluminescence (PL) uniformity on a microscale (**Fig. R5c, d**). For the pristine heterophase film, γ-phase and δ-phase tend to be concentrated in specific regions. By contrast, the alloyed γ/δ-$CsPb(I/Cl)_3$ heterophase film presented much more uniform phase distributions. Besides, temperature-dependent PL results also indicate that changing Cl^- proportions (0-30%) could adjust the relative intensity between $E_{\delta 1}$ and $E_{\delta 2}$, meaning the white light component could be finely regulated, which is consistent with theoretical calculation results.

(3) Carrier dynamics

We applied hyperspectral wide-field microscopy to analyse the carriers' lifetime and behaviour (**Fig. R5e, f**). Carrier lifetime maps also indicate a more uniform phase distribution in γ/δ-$CsPb(I/Cl)_3$ heterophase film. γ-phase and δ-phase had become closely intertwined, which greatly increases the area of the heterophase interface, further resulting in the balanced carrier distribution.

(4) EL spectrum of the devices

Benefiting from the balanced heterophase and carrier distribution, we regulated and then achieved full-spectrum white EL with low blue light component and sunlight-like quality (**Fig. R5h**). In comparison, our previously reported white presented a high blue light component (**Fig. R5g**), which is undesirable and has harmful effects on ecosystems and organisms.

(5) Evolution of EL during the invalidation stage

During the invalidation stage of the device, the intensity of deep-red emission

obviously weakened. Secondly, the emission from TFB layers appeared and continuously strengthened, which was attributed to the degraded and damaged heterophase film resulting in carrier leakage. Thirdly, the evolution in the shape of broadband emission indicated the changes in the carrier recombination region. These results suggested that balanced carriers' distribution and recombination ensured the stability of device operation, carrier recombination region and white EL spectrum (**Fig. R6**).

Finally, we would like to emphasise the new findings and novelty of this work:

(1) We precisely design and regulate heterophase γ/δ-CsPb(Cl/I)$_3$ with multi- and discrete luminescence centres, which could cover the entire visible spectrum (400-780 nm). According to the theoretical calculation results, we designed and optimised the composition of emitting γ/δ-CsPb(I/Cl)$_3$ heterophase film, which could cover the entire visible spectrum (400-780 nm). We observed dual-emission (400-480 nm and 480 nm-650 nm) in δ-CsPbI$_3$ for the first time, which can be combined with γ-CsPbI$_3$ with deep-red emission (650-780 nm) to form full-spectrum white light.

(2) **Alloyed γ/δ-CsPb(I/Cl)$_3$ enables uniform heterophase distribution, balanced flow of charges and tunable spectrum.** Alloyed γ/δ-CsPb(I/Cl)$_3$ brings down the phase-transition temperature between the γ and δ phases and facilitates the stabilisation of the γ phase in thermodynamics, indicating the heterophases could coexist much more uniformly. Besides, alloyed γ/δ-CsPb(I/Cl)$_3$ shows tuneable emission originating from controllable flows of charges between different luminescence centres, which provides the possibility for achieving high-quality full-spectrum white light.

(3) **We achieved white electroluminescence with sunlight-like quality and established a set of index systems for evaluating white light quality.** The match index of the five core indicators to standard sunlight reached 100%, 95%, 99.5%, 99.97% and 99.6%, respectively, representing the closest artificial white electroluminescence to sunlight to date. Besides, such a set of index systems could be helpful for researchers to evaluate the white light quality more objectively.

We believe the **concept of material design**, the **regulation of heterophase distribution**, the **control strategy of carriers in multi- and discrete luminescence centres,** and the **fine regulation of white EL spectrum** would attract broad interest from researchers in the fields of Optoelectronics and Nanotechnology. Besides, the performance of our large-area devices is decent and competitive, as shown in **Table R1**.

As suggested, we have updated the corresponding content in the revised manuscript and highlighted it in yellow.

Page 6: *In brief, the theoretical analysis supports that up to 30% proportion of the Cl^- component enables a more uniform heterophase distribution and feasible lattice twisting, providing the possibility for achieving balanced carrier distribution and tuneable full-spectrum white light (**Fig. 1e**), as observed experimentally later.*

Page 10: *On the other hand, microscopic spatial inhomogeneities of the heterophase distribution could result in unbalanced carrier distribution and non-uniform heterophase emission.*

Page 12: *γ-phase and δ-phase had become closely intertwined, which greatly increases the area of the heterophase interface, further resulting in the balanced carrier distribution and the excellent electrical properties of the film we present below.*

Page 13: *Moreover, changing Cl^- proportions (0-30%) could adjust the relative intensity between $E_{\delta 1}$ and $E_{\delta 2}$, as shown in **Fig. 3h**, **i** and **Fig. S17**, meaning carrier distribution and the white light component could be finely regulated, which is consistent with theoretical calculation results.*

Page 10: *Due to the fine regulation of carrier distribution, the calculated M/P ratio is 1.004 (@6.4 V), which is extremely close to the standard sunlight (M/P ratio = 1) and demonstrates its bio-friendly properties.*

We have also added the discussion of the EL evolution during the device invalidation stage in the revised manuscript and highlighted it in yellow.

Page 16: *The EL evolution during the device invalidation stage suggested that*

*balanced carriers' distribution and recombination ensured the stability of device operation, carrier recombination region and white EL spectrum (**Fig. S21**).*

[FIGURE REDACTED]

Fig. R5 a, b Schematic diagrams of the relative thermodynamic stability between the γ and δ phases for pure $CsPbI_3$ and $CsPb(I/Cl)_3$ systems, respectively. (**Fig. 1e** in the revised manuscript) **c, d** Hyperspectral images of the γ/δ-$CsPbI_3$ and γ/δ-$CsPb(I/Cl)_3$ film ranging from 660 to 700 nm and ranging from 400 to 600 nm, respectively. (**Fig. 3b, c** in the revised manuscript, respectively) **e, f**

Spatially resolved confocal fluorescence-lifetime imaging microscopy of the heterophase film (> 600 nm) (**e**) and the heterophase film (< 600 nm) (**f**). (**Fig. 3d, e** in the revised manuscript, respectively) **g, h** EL of our previous report and this work, respectively. (extracted from the figure in *Nature Photonics **15**, 238-244* (2021) and **Fig. 5j** in the revised manuscript, respectively)

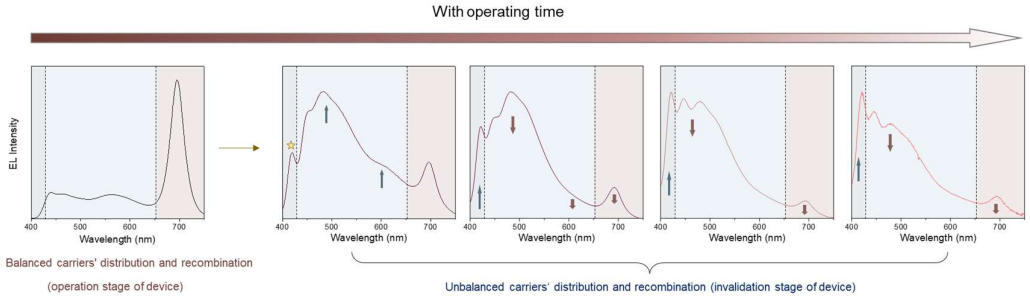

Fig. R6 The evolution of EL during the device invalidation stage. (**Fig. S21** in the revised supporting information)

Table R1 Summary of reported white EL from perovskite (**Table S1** in the revised supporting information)

Emitting layer	Emitting Area	V_{on}	EQE	L_{max}	CIE Coordinates	CRI	CCT	Duv	M/P Ratio	Stability	Ref.
	mm^2	V	%	cd m^{-2}		%	K				
$Cs_2(Ag_{0.6}Na_{0.4})InCl_6$	4	~9	/	~50	/	/	/	/	/	/	13
$CsCu_2I_3$@$Cs_3Cu_2I_5$	4	3	0.05	352.3	(0.33, 0.35)	94	/	/	/	/	14
$CsCu_2I_3$@$Cs_3Cu_2I_5$	4	4.7	0.15	145	(0.32, 0.33)	91.6	/	/	/	238.5 min @100 cd m^{-2}	15
$CsPbCl_3$: Sm	4	> 5	1.2	938	(0.32, 0.31)	93	/	/	/	2.3 min @100 cd m^{-2}	16
α/δ-$CsPbI_3$	4	3.6	6.5	12200	(0.35, 0.43)	~85	/	/	/	230 min @100 cd m^{-2}	17
$CsCu_2I_3$@$Cs_3Cu_2I_5$	3	2.7	3.1	1570	(0.42, 0.47)	/	/	/	/	/	18
$Cs_2AgIn_{0.9}Bi_{0.1}Cl_6$	3	10.5	0.08	158	(0.32, 0.33)	/	/	/	/	48.5 min @8 cd m^{-2}	19
$Cs_2AgIn_xBi_{1-x}Cl_6$	4	5.5	0.013	58	/	/	/	/	/	/	20
$Cs_3Cu_2I_5$	3	3.5	0.71	2116	(0.37, 0.40)	91	4453	/	/	/	21
$Cs_2AgIn_xBi_{1-x}Cl_6$	2	3.1	0.7	3163	(0.33, 0.33)	87.7	5702	/	/	/	22
γ/δ-$CsPb(Cl/I)_3$	100	3.2	2.54	4536	(0.33, 0.33)	95	5835	-0.0003	1.004	220 min @164 cd m^{-2}	This work

Comment 3: How about the performance of small-area devices? The authors used nearly identical spin coating parameters in this study. Why, then, did they achieve better large-area films in this work compared to their previous study?

Response: Thank you for your suggestions. As suggested, we have demonstrated the performance of small-area WLED based on the alloyed heterophase film (**Fig. R7**), which was comparable with our previous report and represented the best performance of white LED in the field (EQE> 6%, Luminance>10^4 cd m^{-2}).

Besides, considering that fabricating a large-area plane light source is of practical significance for lighting applications, we focused on the photoelectric characteristics of large-area heterogeneous films in this work. We designed and optimised the heterophase composition — alloyed γ/δ-$CsPb(I/Cl)_3$ film. The alloyed γ/δ-$CsPb(I/Cl)_3$ film showed more balanced heterophase and carrier distribution compared with unalloyed heterophase film (previous report), enabling sunlight-like large-area white EL.

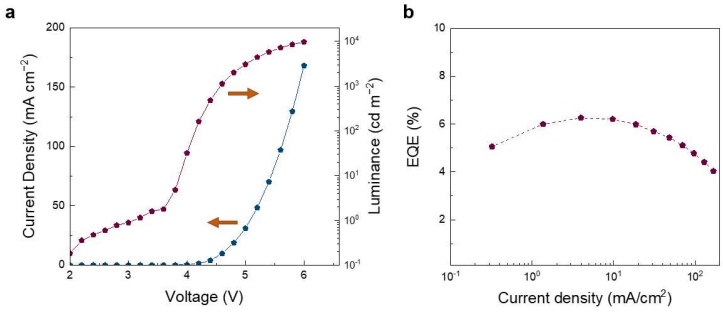

Fig. R7 The EL performance of small-area WLED based on alloyed heterophase film.

Replies to Reviewer #2

Comments to the Author:

We thank the authors for their efforts in addressing our comments. However, after reviewing the revised manuscript and the responses to the reviewers, I still have some concerns.

Comment 1: The authors mention that different instruments were used to test the white LEDs and $CsPbI_3$-based LED devices. We strongly recommend using the same testing instrument for comparison, as this may help to eliminate abnormal peaks.

Response: We appreciate your constructive suggestions and applied the same testing instrument for comparison. As shown in **Fig.R8**, we successfully eliminated the abnormal peaks around 690 nm.

We have updated the corresponding figure (**Fig. R9**) in the revised manuscript.

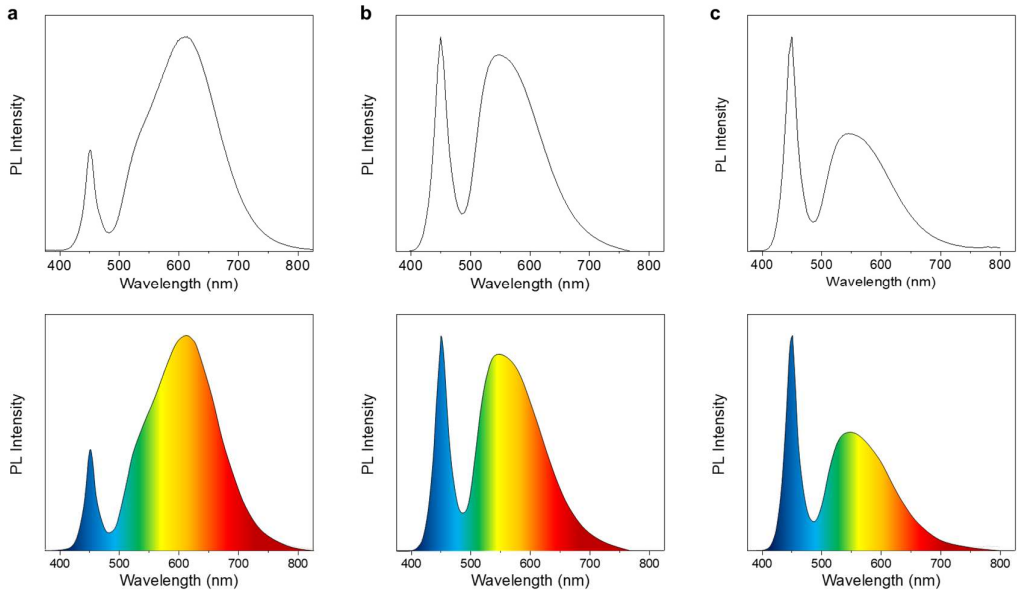

Fig.R8 a, The normalised spectrum of three commercial WLED-1. **b**, The normalised spectrum of three commercial WLED-2. **c**, The normalised spectrum of three commercial WLED-3.

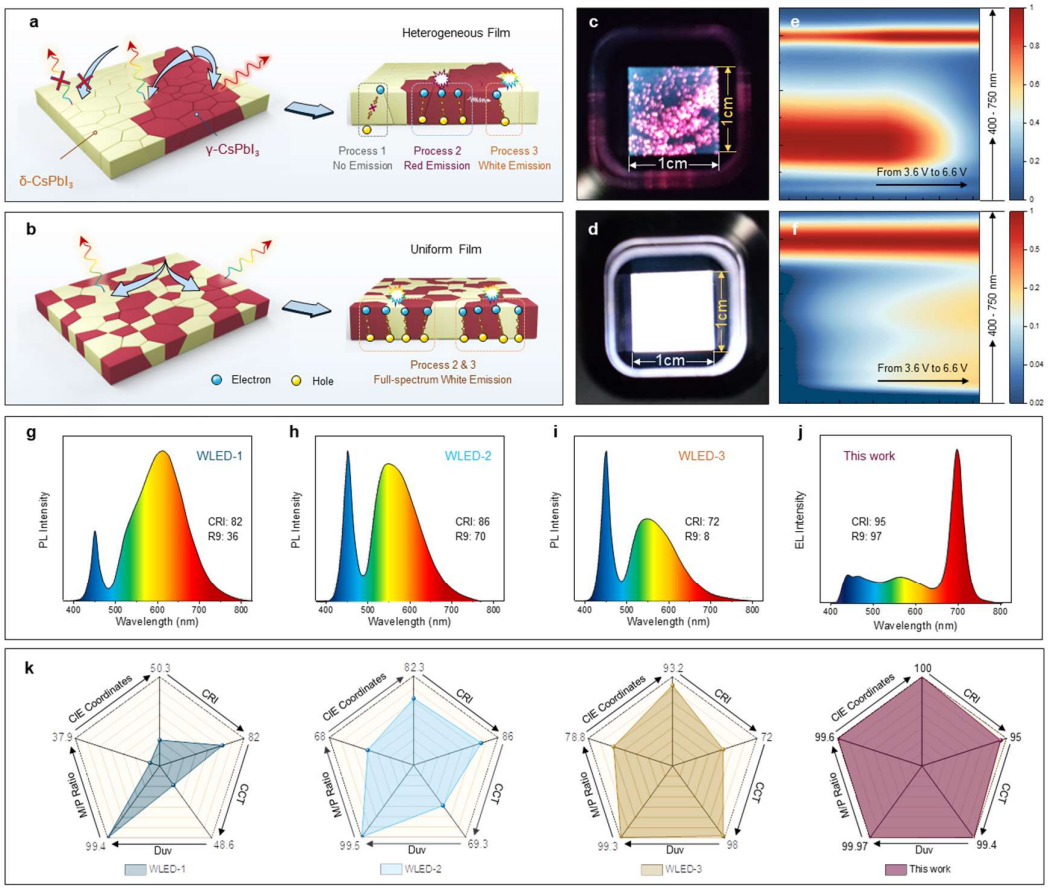

Fig.R9 The mechanism of carrier transport and recombination in the large-area WLEDs. **a,** Demonstration of carrier transport and carrier recombination process in the control device, where Process 1 dominates the whole process. **b**, Demonstration of carrier transport and carrier recombination process in the target large-area WLED, where Process 3 plays a crucial role. **c**, The photograph of the control large-area WLED, showing heterogeneous multicolour EL. **d**, The photograph of the target large-area WLED, showing uniform and pure white EL. **e**, Normalised EL spectra of the control device as applied bias increasing from 3.6 V to 6.6 V. **f**, Normalised EL spectra of the target WLED as applied bias increasing. **g-i**, The normalised spectrum of three commercial WLEDs, where blue light acts as the excitation source. **j,** The normalised EL spectrum of WLED with low blue-light component. **k**, Comparison of match index of representative commercial WLEDs and this work. (**Fig.5** in the revised manuscript)

<u>Comment 2:</u> The lifetime of white LEDs is critical. According to Figure R4, there is no obvious change in intensity or spectral shape, indicating that the device has good

operating stability. Typically, the duration of the lifetime test for LEDs should be extended to T_{50}. We recommend extending the testing duration and comparing the results with previously reported works in terms of lifetime.

Response: Thank you for your suggestion. We have extended the testing duration and added the operational lifetime of reported works in **Table R2**. It can be found that our device showed the best operational stability performance among them.

We have updated the corresponding figure and table (**Fig. R10** and **Table R2**) in the revised supporting information.

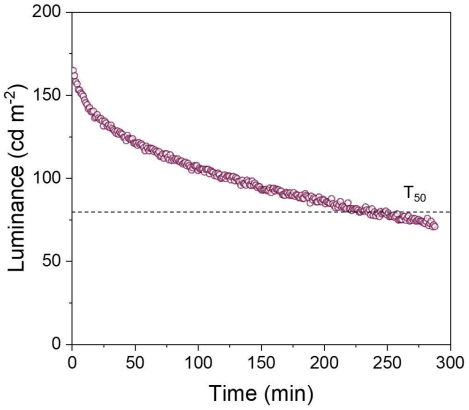

Fig. R10 The typical Pe-WLED lifetime (T_{50}) is about 220 min when monitoring the luminance under an initial luminance of 164 cd m^{-2}. (**Fig. S20** in the revised supporting information)

Table R2 Summary of reported white EL from perovskite (**Table S1** in the revised supporting information)

Emitting layer	Emitting Area	V_{on}	EQE	L_{max}	CIE Coordinates	CRI	CCT	Duv	M/P Ratio	Stability	Ref.
	mm^2	V	%	cd m^{-2}		%	K				
$Cs_2(Ag_{0.6}Na_{0.4})InCl_6$	4	~9	/	~50	/	/	/	/	/	/	13
$CsCu_2I_3$@$Cs_3Cu_2I_5$	4	3	0.05	352.3	(0.33, 0.35)	94	/	/	/	/	14
$CsCu_2I_3$@$Cs_3Cu_2I_5$	4	4.7	0.15	145	(0.32, 0.33)	91.6	/	/	/	238.5 min @100 cd m^{-2}	15
$CsPbCl_3$: Sm	4	> 5	1.2	938	(0.32, 0.31)	93	/	/	/	2.3 min @100 cd m^{-2}	16
α/δ-$CsPbI_3$	4	3.6	6.5	12200	(0.35, 0.43)	~85	/	/	/	230 min @100 cd m^{-2}	17
$CsCu_2I_3$@$Cs_3Cu_2I_5$	3	2.7	3.1	1570	(0.42, 0.47)	/	/	/	/	/	18
$Cs_2AgIn_{0.9}Bi_{0.1}Cl_6$	3	10.5	0.08	158	(0.32, 0.33)	/	/	/	/	48.5 min @8 cd m^{-2}	19
$Cs_2AgIn_xBi_{1-x}Cl_6$	4	5.5	0.013	58	/	/	/	/	/	/	20
$Cs_3Cu_2I_5$	3	3.5	0.71	2116	(0.37, 0.40)	91	4453	/	/	/	21
$Cs_2AgIn_xBi_{1-x}Cl_6$	2	3.1	0.7	3163	(0.33, 0.33)	87.7	5702	/	/	/	22
γ/δ-$CsPb(Cl/I)_3$	100	3.2	2.54	4536	(0.33, 0.33)	95	5835	-0.0003	1.004	220 min @164 cd m^{-2}	This work

Comment 3: The authors claim: "The α-phase will spontaneously undergo a phase transition to the β-phase, then to the γ-phase, and finally to the δ-phase at room temperature," and "Joule heat generation during operation promotes the phase transition from the γ-phase to the δ-phase." So, will the γ/δ-$CsPbI_3$ film eventually transform entirely into the δ-phase during long-term operation? Please provide more experiment results and discussion.

Response: Thank you for your suggestions. In the last round of revision, we found that there were no obvious changes in intensity or spectral shape during the operation stage of the device. In this round of revision, we have studied the evolution of EL during the invalidation stage of the device (**Fig. R11**), as suggested.

During the invalidation stage of the device, the intensity of deep-red emission obviously weakened. Secondly, the emission from TFB layers appeared and continuously strengthened, which was attributed to the degraded phase and damaged

heterophase film inducing carrier leakage. Thirdly, the evolution in the shape of broadband emission indicated the changes in the carrier recombination region. These results suggested that balanced carriers' distribution and recombination ensured the stability of device operation, carrier recombination region and white EL spectrum.

As suggested, we have added the discussion of the EL evolution during the device invalidation stage in the revised manuscript and highlighted it in yellow.

Page 16: *The EL evolution during the device invalidation stage suggested that balanced carriers' distribution and recombination ensured the stability of device operation, carrier recombination region and white EL spectrum (**Fig. S21**).*

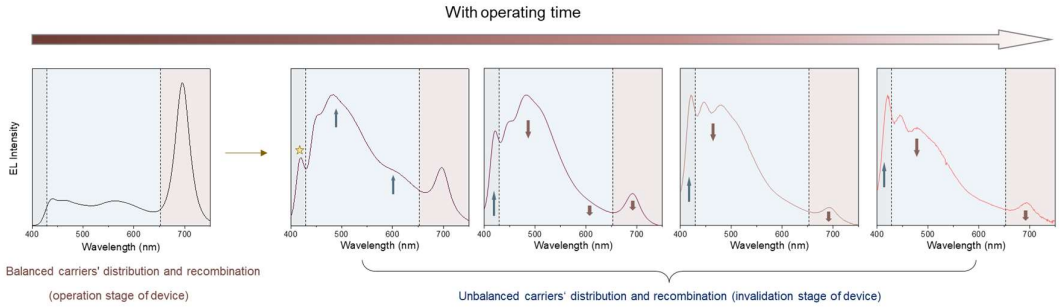

Fig. R11 The evolution of EL during the device invalidation stage. (**Fig. S21** in the revised supporting information)

We appreciate reviewers' helpful comments and suggestions and have replied to them point by point in the following content. For clarity, reviewers' original comments and our response are in blue fonts, and the changes we made to the main text are quoted in *red fonts*. We have also highlighted the corresponding modifications in yellow in the revised manuscript.

Replies to Reviewer #1

Comments to the Author:

In the response letter and the revised manuscript, the authors have addressed my concerns. I suggest the authors add the data of small-area devices in the supplementary information.

Response: We appreciated your suggestion, and we have added the **Fig. R1** in the revised supporting information.

Page 16: *The target device showed an EQE of 2.54% and a CE of 3.46 cd A^{-1} with an emitting area of 100 mm^2 (see **Fig. S20** for typical device performance with an emitting area of 4 mm^2), representing the first large-area WLED to date to the best of our knowledge (**Table S1** and **Table S2**).*

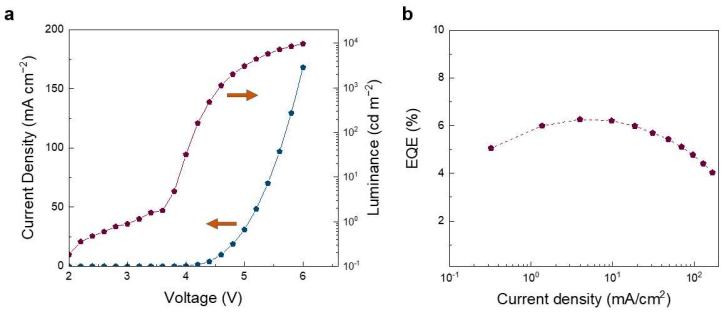

Fig. R1 The EL performance of typical small-area WLED with an emitting area of 4 mm^2. (**Fig. S20** in the revised supporting information)

Replies to Reviewer #2

Comments to the Author:

We thank the authors for their efforts in addressing our comments. However, after reviewing the revised manuscript and the responses to the reviewers, I still have some concerns.

Comment 1: The authors presented the stability result, showing a T_{50} of 220 minutes. Based on this result, we have concerns about the EL spectrum evolution in Fig. S25, which indicates no degradation in EL intensity. Please clarify the discrepancy between these two results.

Response: We appreciate your comment. In order to better show the relative EL intensity and analyse the ratio of the two phases, we previously normalised the EL spectrum (**Fig. R2**). Thus, there seems to be no obvious degradation in EL intensity.

As suggested, we have shown the absolute EL intensity (**Fig. R3a**) and the relative EL intensity together (**Fig. R3b**). Besides, we have updated the caption to avoid confusion.

Page 16: *The specific half-lifetime (T_{50}) was ~220 min (L_0 = 164 cd m^{-2}), showing decent operational stability (**Fig. S21**) and spectrum stability (**Fig. S22**).*

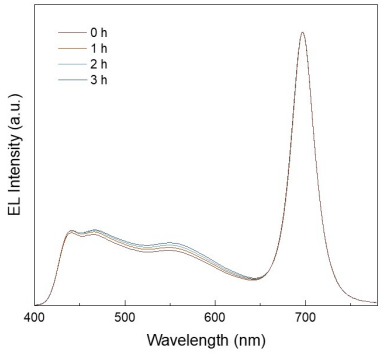

Fig. R2 Normalised EL spectrum with device operating.

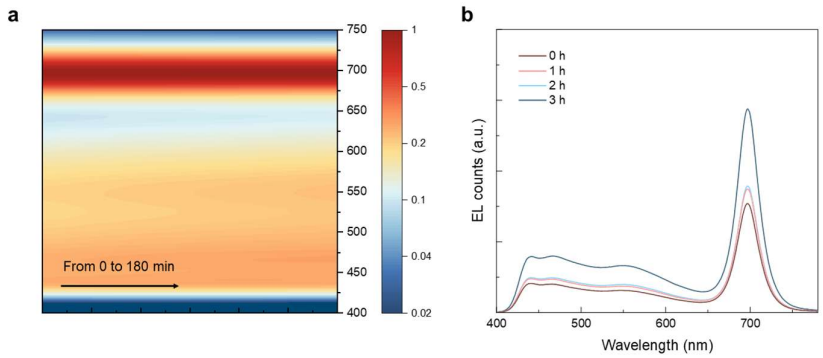

Fig. R3 a, Normalised EL intensity with device operating, showing steady spectral shape. **b**, Absolute EL intensity spectrum with device operating.

Comment 2: In the revised manuscript, the authors mentioned the device invalidation stage. However, they did not specify when the invalidation occurred—was it before or after T_{50}? Please add spectrum change data over the entire operating time.

Response: We apologise for not being more specific about the test condition. The device invalidation stage occurred after T_{20} (luminance decreased to 20% of the initial luminance), which was often overlooked for LED with single and narrow emission in other reports. Our Pe-WLED has multi- and discrete emissions, and the carriers' distribution, transport and recombination processes are complicated. Thus, we examined the device's EL spectrum after its luminance decreased to 20% of the initial luminance (device invalidation stage) to explore the roots of device invalidation (**Fig. R4**). We accelerated the test to skip the intermediate stage and collect the data under the device invalidation stage. The left column of **Fig. R4** showed the normalised EL intensity evolution of the device under steady state operation (before T_{50}), while the right column of **Fig. R4** showed the normalised EL intensity evolution of the device during the device invalidation stage (after T_{20}). We analysed the device invalidation mechanism in detail in our response to the following **Comment 3**.

As suggested, we have updated the figure and described the test condition clearly.

Page 16: *To explore the device invalidation mechanism and find strategies for performance boost at the root, we next examined the device's EL spectrum after its*

*luminance decreased to 20% of the initial luminance (device invalidation stage) (**Fig. S23**).*

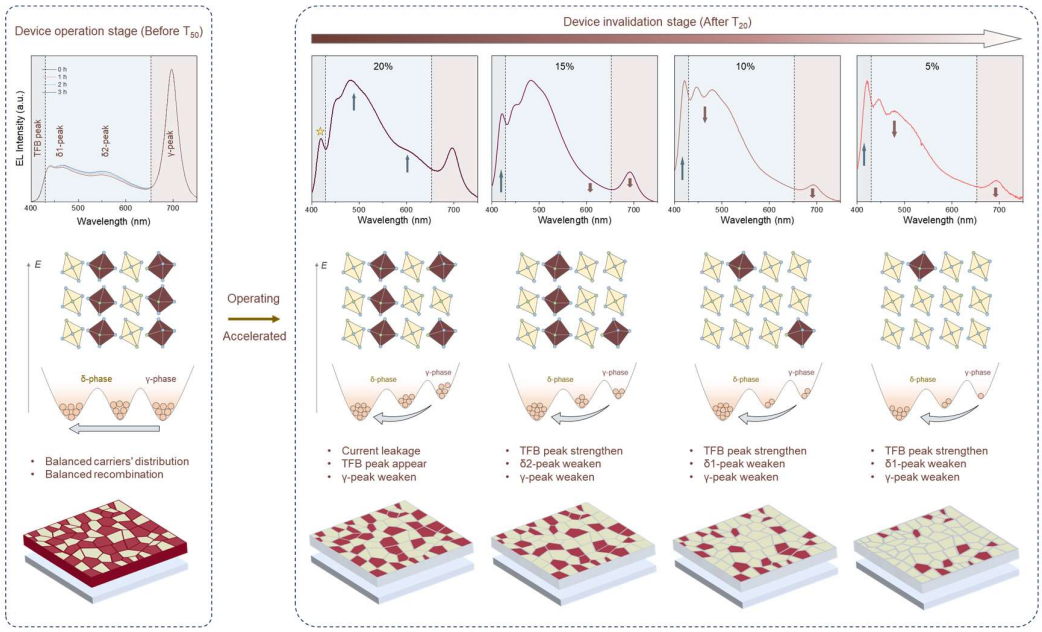

Fig. R4 The EL spectrum, carrier distribution and heterophase composition evolution during the steady-state device operation stage and device invalidation stage (**Fig. S23** in the revised supporting information)

Comment 3: The authors have still not addressed our question regarding the phase transition during operation. Please investigate and test the phase transition during continuous operation, as this will help elucidate the mechanism of device invalidation.

Response: We appreciate your constructive suggestions. We analysed the phase transition and charge transfer direction by measuring the EL shape evolution and relative EL intensity of different peaks, as shown in updated **Fig. S23** (**Fig. R5**). We collected data during the typical steady-state operation stage (before T_{50}) and device invalidation stage (after T_{20}). During the steady-state operation stage, the device showed steady spectral shapes while the relative intensity of broadband emission from δ-phase enhanced. This indicated the balanced carriers' distribution and recombination between different energy levels of heterophases and a slight phase transition from the γ-phase to the δ-phase.

During the device invalidation stage, the carriers' distribution and recombination showed worsening unbalance, and the phase transition accelerated. Firstly, we observed a peak from TFB layers (~425 nm) appeared and continuously strengthened, which was attributed to the degraded phase and damaged heterophase film inducing current leakage. Secondly, the intensity of deep-red emission from the γ-phase continuously weakened with the intensity of emission from the δ-phase enhancing, indicating the generated Joule heat during device operation promoted phase transition from γ-phase to δ-phase constantly. Thirdly, the evolution in the shape of white EL suggested how the changes or energy flows under the unbalanced heterophase system: charge injection into the γ-phase, γ to δ-phase ($E_{\delta 2}$), and δ-phase ($E_{\delta 2}$) to δ-phase ($E_{\delta 1}$), which is also consistent with temperature-dependent PL results. Thus, the EL evolution during the device invalidation stage suggested that balanced carriers' distribution and recombination ensured the stability of device operation, carrier recombination region and white EL spectrum. Hence, we expect more reasonable designs of the heterophase structure, composition and distribution could enhance the carrier recombination, coupled with more rational device structure designs, further improving the efficiency and stability of the devices.

Page 16: *Up to now, the EQEs of reported perovskite WLED are usually less than 1% with limited operational stability, and there is much room for improving device performance to satisfy future commercial applications (**Table S1**).*

Page 16: *To explore device invalidation mechanism and find strategies for performance boost at the root, we next examined the device's EL spectrum after its luminance decreased to 20% of the initial luminance (device invalidation stage) (**Fig. S23**). Firstly, the emission from TFB layers (~425 nm) appeared and continuously strengthened, which was attributed to the degraded phase and damaged heterophase film inducing current leakage. Secondly, the intensity of deep-red emission from the γ-phase continuously weakened with the intensity of emission from the δ-phase enhancing, indicating the generated Joule heat during device operation promoted phase transition from γ-phase to δ-phase constantly (a similar phenomenon was also observed during*

the device operation stage). Thirdly, the evolution in the shape of white EL suggested how the changes or energy flows under the unbalanced heterophase system: charge injection into the γ-phase, γ to δ-phase ($E_{\delta 2}$), and δ-phase ($E_{\delta 2}$) to δ-phase ($E_{\delta 1}$), which is also consistent with temperature-dependent PL results. Thus, the EL evolution during the device invalidation stage suggested that balanced carriers' distribution and recombination ensured the stability of device operation, carrier recombination region and white EL spectrum. In brief, beyond drawing reference from reported performance-improving strategies for monochromatic perovskite LEDs, we expect more reasonable designs of the heterophase structure, composition and distribution could enhance the carrier recombination, coupled with more rational device structure designs, further improving the efficiency and stability of the devices.

Page 19: *With the increased applied bias, an increase in broadband emission corresponding to the δ-phase was observed (**Fig. 5f**), signalling that the electric field could facilitate more charges to inject into the δ-phase through heterophase interphase, which is consistent with the conclusions drawn from EL evolution during the device invalidation stage (**Fig. S23**). The appearance of the TFB peak for the control device can be attributed to current leakage caused by the heterogeneous surface of the control heterophase film.*

Page 13: *The excited states will first transfer to the self-trapped state through ultrafast excited-state structural reorganisation, releasing lattice distortion and broadband emission ($E_{\delta 2}$). Then the carriers transfer to the exciton level ($E_{\delta 1}$) with energy compensation, and finally fall back to the ground state (**Fig. S16**). Furthermore, temperature-dependent PL results also indicate that higher temperatures could promote the transfer of carriers between heterophases (**Fig. 3h, i**).*

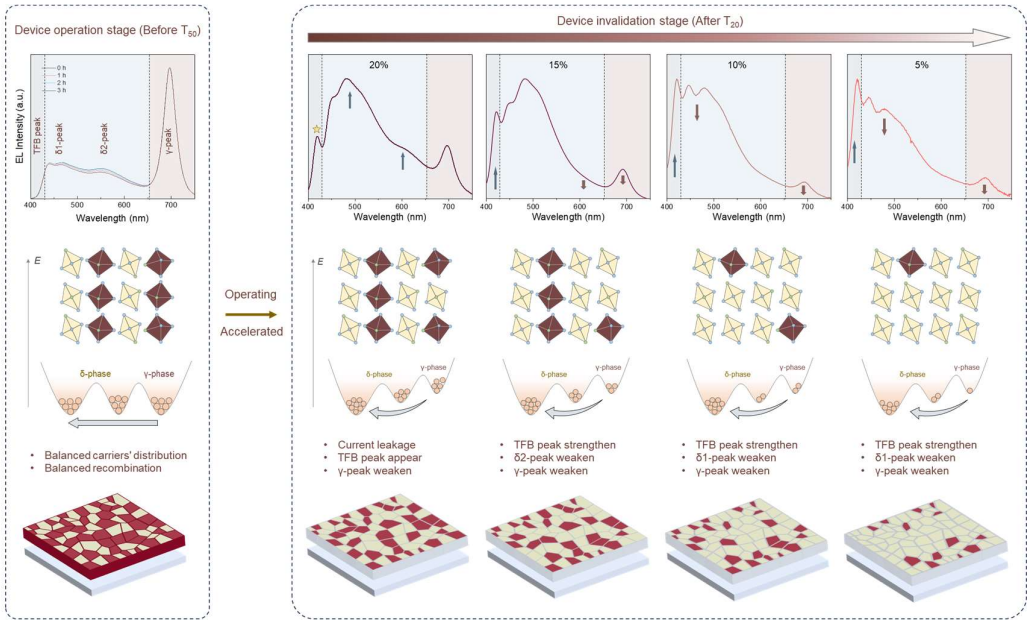

Fig. R5 The EL spectrum, carrier distribution and heterophase composition evolution during the steady-state device operation stage and device invalidation stage (**Fig. S23** in the revised supporting information)

Comment 4: The T_{50} of the device remains far from meeting the requirements for practical applications. Please include a more in-depth discussion on this point and provide suggestions or strategies for improving the stability of the device.

Response: We agree with the reviewer that perovskites are more likely to suffer from chemical, phase and optical degradation, leading to an operating lifetime of only tens or hundreds of hours, which is regarded as uncertainty and risk for further commercialisation. We will discuss it from the following aspects.

(1) Efficiency

In the current state, the EQEs of reported perovskite WLED are usually less than 1% or even 0.1%. Low photoelectric conversion efficiency originates from unbalanced carrier recombination, which leads to excess carriers and too much Joule heat generation, ultimately affecting the device's operational time. Thus, improving efficiency could enhance the operational stability of the device. The related work about improving efficiency has made some progress in monochromatic perovskite LEDs,

such as Lewis acid/base passivating, cross-linking and interfacial modification strategies, which is of reference significance to perovskite WLEDs.

(2) Materials design

Different from monochromatic perovskite, materials with multi- and discrete luminescence centres have much more complex processes in the distribution and recombination of carriers. Thus, we should design the phase structure, composition and distribution more reasonably combined with theoretical calculations, achieving more balanced and efficient carrier injection into different phases. We also expect this work could offer insights to researchers in designing materials with multi- and discrete luminescence centres for full-spectrum white EL.

(3) Phase degradation

It is reported that $CsPbI_3$ usually undergoes a spontaneous phase transition from a black photoactive α/β/γ-phase to a yellow photoinactive δ-$CsPbI_3$ phase. As discussed in this work, the white EL spectrum could keep steady under balanced carrier injection and recombination. As the device operates, a phase transition occurs but does not significantly change the white EL spectrum.

(4) Device design and structure optimisation

The matched energy level and structure of each functional layer are also important for device stability. Thus, we could select and modify the transport layer to match well with the white emitting layer.

Combining the discussion above and the analysis of the device invalidation, we expect a more reasonable design of the heterophase structure, composition and distribution could enhance the carrier recombination, coupled with more rational device structure designs, further improving the efficiency and stability of the devices.

As suggested, we have added the discussion in the revised manuscript and highlighted it in yellow.

Page 16: *Up to now, the EQEs of reported perovskite WLED are usually less than 1%*

*with limited operational stability, and there is much room for improving device performance to satisfy future commercial applications (**Table S1**).*

Page 16: *To explore the device invalidation mechanism and find strategies for performance boost at the root, we next examined the device's EL spectrum after its luminance decreased to 20% of the initial luminance (device invalidation stage) (**Fig. S23**).*

Page 16: *In brief, beyond drawing reference from reported performance-improving strategies for monochromatic perovskite LEDs, we expect more reasonable designs of the heterophase structure, composition and distribution could enhance the carrier recombination, coupled with more rational device structure designs, further improving the efficiency and stability of the devices.*